Reconfigurable intelligent surface passive beamforming enhancement using unsupervised learning

Intisar Al-Shaeli, Ismail Sharhan Hburi, Ammar A. Majeed
Department of Electrical Engineering, Faculty of Engineering, Wasit University, Wasit Province, Iraq

Article Info

Article history:

Received Feb 25, 2022
Revised Sep 2, 2022
Accepted Sep 20, 2022

Keywords:

6G networks
Beamforming neural network
Massive multi-input multi-output
Reconfigurable intelligent surfaces
Unsupervised learning

ABSTRACT

Reconfigurable intelligent surfaces (RIS) is a wireless technology that has the potential to improve cellular communication systems significantly. This paper considers enhancing the RIS beamforming in a RIS-aided multiuser multi-input multi-output (MIMO) system to enhance user throughput in cellular networks. The study offers an unsupervised/deep neural network (U/DNN) that simultaneously optimizes the intelligent surface beamforming with less complexity to overcome the non-convex sum-rate problem difficulty. The numerical outcomes comparing the suggested approach to the near-optimal iterative semi-definite programming strategy indicate that the proposed method retains most performance (more than 95% of optimal throughput value when the number of antennas is 4 and RIS's elements are 30) while drastically reducing system computing complexity.

Corresponding Author:

Intisar Al-Shaeli
Department of Electrical Engineering, Faculty of Engineering, Wasit University
Hay Al-Rabea Road, Al-Kut District, Wasit Province, Iraq
Email: intisark302@uowasit.edu.iq

1. INTRODUCTION

Reconfigurable intelligent surface (RIS) has been intended as a potentially transformative technology capable of lowering power usage and enhancing network throughput by artificially altering the propagation environment of electromagnetic waves (EM) [1]. RISs possess the enormous prospective to change wireless network design and enable the creation of intelligent radio environments [2]. This ability occurs when merged with other fifth-generation prospective technologies, such as non-orthogonal multiple access (NOMA) systems [3], terahertz cellular systems, multi-input multi-output (MIMO) systems [4], and wireless networks powered by artificial intelligence (AI) [5], [6]. Several essential characteristics that distinguish RIS from recent technologies are highlighted in [7]. These characteristics contain specific design constraints imposed by the RIS elements' near-passive nature. These qualities open up new possibilities for modifying the wireless environment, boosting the efficiency of radio wave use, extending coverage, transferring energy, locating, and enhancing spatial capacity density [8] while improving energy consumption [9]. Simultaneously, these characteristics introduce new difficulties in designing RIS-aided cellular networks, including the transmission of information inside a RIS-enabled environment, enhancement of the RIS configuration with restricted information, resource allocation, and the optimization of the network in such cellular systems, as provided in [10].

Furthermore, machine learning (ML) techniques and deep learning (DL) have emerged as valuable tools for dealing with massive amounts of data [11], exponential non-convex challenges that are mathematically difficult, and computationally intensive challenges [12], [13]. DL-based techniques have been employed in various cellular systems, including physical layer communications [14] and "resource allocation" [15]. Inspired by the prospect of using DL for complex maximization problems, in study [1] the authors used the DL technique to construct the RIS beamforming matrices with restricted channel state information (CSI). The active/passive beamforming was intended to enhance the secrecy performance of reflective RIS-assisted MIMO networks with a single genuine receiver and a single eavesdropper in [16], [17]. In the scope of RIS-aided communication systems, authors in references [18], [19] proposed a supervised learning strategy in which a deep neural network (DNN) is learned offline to demonstrate an implicit connection among both measured coordinate information and the RIS's phase configuration. However, a significant difficulty for supervised learning is obtaining labels. Gao *et al.* [20] achieved the ideal labels using extensive search, which is cost-prohibitive in practice, especially when many training examples are necessary. Gao *et al.* [20] introduced a modified DNN for single-user RIS-assisted MIMO networks trained offline using the unsupervised learning approach. This study produces a structure that can estimate real-time when utilized online. They showed through simulation that the proposed mechanism significantly decreases computation complexity in comparison to the traditional suboptimal scheme that employs a semi-definite relaxation method. Song *et al.* [21] introduced a novel two-stage structure to optimize the transmit beamforming and the RIS phase shift matrix together and, consequently, the sum rate of all users. Based on the characteristics of this problem, they carefully customized network layers, features, and loss functions.

The current study proposed an efficient and low-cost DNN structure to improve the passive beamforming vectors in RIS-assisted MIMO systems with a power limitation target. A particular emphasis is placed on developing a customized DNN construction for the RIS beamforming design challenge and selecting a set of specific characteristics for the training process. To eliminate the labeling complexity associated with supervised learning, we suggest using the "unsupervised learning" technique for RIS beamforming design in this study, like [22], [23]. Different from the work in [20], the suggested structure of the neural network can deal with more complicated multiuser scenarios to optimize the system throughput under the constraint of the access point (AP) maximum allowed transmitting power. In addition, different from the approach employed in [21], our proposed architecture considers three channels at the network input instead of two-channel. These are direct, reflected, and AP_RIS channels which make the scheme appropriate for more realistic environments and improve the feature extraction of the network.

The following summarizes the study contributions. At the start point, the study offers a framework for the multiantenna method that utilizes a DNN to select a beamformer with the optimal spectral performance while minimizing transmission power. Following that, numerical experiments were undertaken to test the suggested system performance, which revealed that the proposed design offers a critical performance boost compared to standard beamforming approaches. This article was structured: section 1 introduction. Section 2 system model and formulation of the problem. Section 3 DNN structure. In section 4, numerical results were discussed. Conclusion the paper is done in section 5. Notations: the capital letters like (M, N) denote scalar constants. Small latter like ($k,\ldots r$) denote scalar variables. Vectors are represented by bold small latter like ($\boldsymbol{h}$), where the h_k means the k^{th} element of h. Capital bold latter implies matrix-like $\boldsymbol{F}$. *Diag (·)* denotes the diagonal operation. We use $tr\ (.)$, $(.)\ H$, C, indicates the matrixes' trace, conjugate transpose (Hermitian), and complex matrix, respectively.

2. SYSTEM MODEL AND FORMULATION OF THE PROBLEM

Based on our previous work in [24], which depends on the traditional iterative approach to cope with the transmission/reflection beamforming design problem, the current work follows an entirely different simple path to meet the proposed goal of this study by employing an artificial neural approach. Specifically, we consider a RIS-enhanced multiuser MIMO wireless system, as shown in Figure 1. that consists of |Ap| numbers of APs configured with M antenna elements servicing the downlink of single-antenna K users. The AP is aided by R numbers of RIS, each containing N reflective elements. Without losing of generality, we consider that all channels' channel state information (CSI) is precisely known at the AP and RIS. The direct path to the K^{th} user is expressed through a channel matrix with complex vectors, $\boldsymbol{F}a,k \in \mathbb{C}\ N\times K$. Without lossing of generality, we consider that all channels' CSI is precisely known at the AP and RIS. The surface-user path is implied by $\boldsymbol{h}r,k \in \mathbb{C}\ N\times 1$, while the MIMO AP-RIS links channel matrix is denoted as $\boldsymbol{G}a,r \in \mathbb{C}\ M\times N$. Diagonal matrix $\Phi r \in \mathbb{C}\ N\times N$ is the received signal phase shift at the RIS, where $\boldsymbol{\Phi} r=\sqrt{\eta}$ diag ($\boldsymbol{\Phi}$ r1,… $\boldsymbol{\Phi}$ rn), ∀r ∈ R. Theoretically, an element's reflection amplitude can be tuned for diverse tasks, e.g., performance optimization and channel acquisition [25]. Nevertheless, in practice, it is expensive to consider an independent controller of the phase shift and amplitude of the reflection simultaneously.

Consequently, an individual element is typically considered to optimize the signal reflection as simplicity. For the motive of the simplicity of practical execution, we assume a discrete value (finite-number) for the RIS's element phase shifts. It is worth noting that the discrete phase shifter's quantization loss significantly grows as N increases. For scenarios with a big N, we choose high-order quantization to reduce the discrete phase shifter's quantization loss. If we employ b-bits to characterize the phase-shift levels, then the number of these levels will be 2^b [26]. For simplicity, we assume uniform-quantization for the discrete phase-shifts levels in the range [0; 2π)]. To this end, at each RIS element, the discrete phase shift values set will be,

$$\boldsymbol{\Phi}_{r,n} \in \left\{0, \frac{\pi}{2^{b-1}}, \dots, (2^b - 1)\frac{\pi}{2^{b-1}}\right\}, \quad \forall \mathrm{r} \in \mathrm{R}, \forall \mathrm{n} \in \mathrm{N} \tag{1}$$

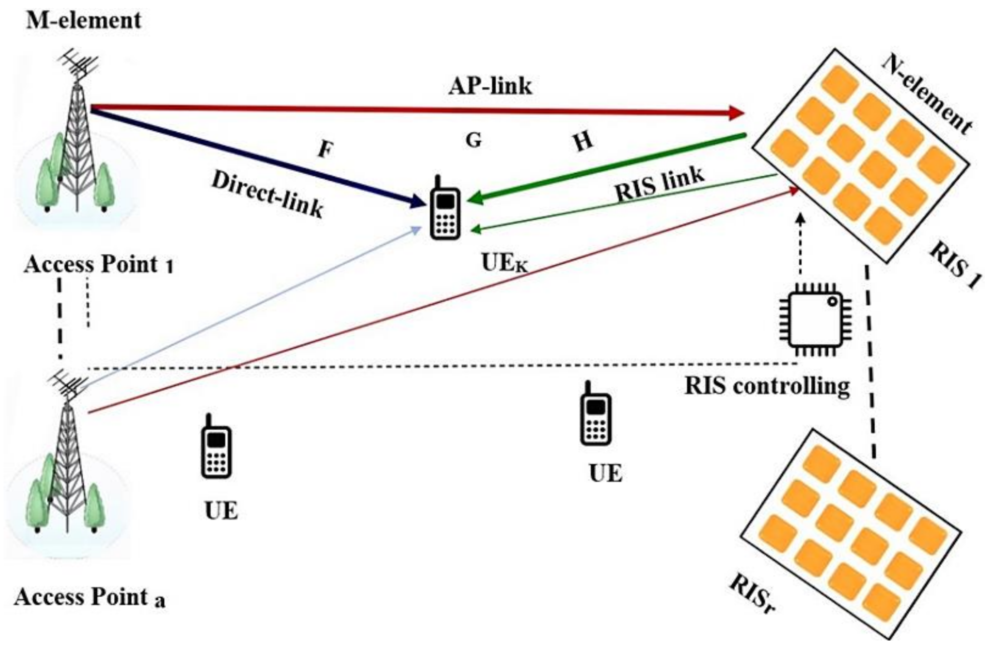

Figure 1. Model of the proposed multiple RISs schemes

At the AP, the transmitted baseband signals are represented,

$$x = \sum_{k=1}^{K} \boldsymbol{V}_{a,k} S_k \tag{2}$$

where S_k is the transmitted symbol to the k^{th} user, ($k=1, \dots K$) [9], and $\boldsymbol{V}_{a,k}$ is a baseband beamformer vector for the k^{th} user, $\mathbf{V}_{a,k} \in \mathbb{C}^{M\times K}$ for $m=1, \dots M$. Using the system model discussed above, the received signal at the k^{th} user can be described in the following manner,

$$y_k = \underbrace{\sum_{a\in|Ap|} \boldsymbol{F}_{a,k}^H \boldsymbol{V}_{a,k} S_k + \sum_{a\in|Ap|} \sum_{r\in|R|} \boldsymbol{H}_{r,k}^H \boldsymbol{\Phi}_r^H \boldsymbol{G}_{a,r} \boldsymbol{V}_{a,k} S_k}_{useful-signal} + \underbrace{\sum_{a\in|Ap|} \sum_{\substack{i\in|K|\\ i\neq k}} \boldsymbol{F}_{a,k}^H \boldsymbol{V}_{a,i} S_i + \sum_{a\in|Ap|} \sum_{\substack{i\in|K|\\ i\neq k}} \sum_{r\in|R|} \boldsymbol{H}_{r,k}^H \boldsymbol{\Phi}_r^H \boldsymbol{G}_{a,r} \boldsymbol{V}_{a,i} S_i}_{interference-signal} + \boldsymbol{n}_k \tag{3}$$

where $\mathbf{n}_k \sim \mathrm{CN}(0, \sigma^2)$ is the additive white Gaussian noise at the receiver for the k-th user, and the useful-signal includes both direct Ap-user and indirect AP-RIS-user paths. Next, if we use the symbols $\boldsymbol{\Phi}, \mathbf{G}_r$ and $\mathbf{V}_k$, for respectively, diag.$\{\boldsymbol{\Phi}_1, \boldsymbol{\Phi}_2, \dots \boldsymbol{\Phi}_R\}$, ${\mathbf{G}_r}^T = [{\mathbf{G}_{1,r}}^T, {\mathbf{G}_{2,r}}^T, \dots {\mathbf{G}_{AP,r}}^T]$, and ${\mathbf{V}_k}^T = [{\mathbf{V}_{1,k}}^T, {\mathbf{V}_{2,k}}^T, \dots {\mathbf{V}_{AP,k}}^T]$, the last expression for the received signal y_k in (3) may be simplified into, $\sum_{a\in|Ap|} \sum_{i\in|K|} \left(\boldsymbol{F}_{a,k}^H + \boldsymbol{H}_k^H \boldsymbol{\Phi}_r^H\right) \boldsymbol{V}_i S_{a,i} + \boldsymbol{n}_k$. In addition, if we use the notation $\mathbf{Q}_k$ to denote the equivalent channel for the useful signal such that,

$$\mathbf{Q}_k^H = \mathbf{F}_k^H + \sum_{r\in|R|} \mathbf{H}_k^H \boldsymbol{\Phi}_r^H \mathbf{G}_r \tag{4}$$

Then, the received signal and signal to interference plus noise ratio (SINR) at user k are expressed, respectively,

$$y_k = \sum_{i=1}^{k} \boldsymbol{Q}_k^H \boldsymbol{V}_i S_i + \boldsymbol{n}_k \tag{5}$$

$$\Gamma_k(\boldsymbol{\Phi}, \boldsymbol{V}) = \frac{\boldsymbol{V}_k^H \boldsymbol{Q}_k \boldsymbol{Q}_k^H \boldsymbol{V}_k}{\sum_{\substack{i\in|K| \\ i\neq k}} \boldsymbol{V}_i^H \boldsymbol{Q}_k \boldsymbol{Q}_k^H \boldsymbol{V}_i + \boldsymbol{n}_k} \tag{6}$$

To this end, the sum rate (*Nat/s/Hz*) per user k is shown as (7),

$$R_t = \sum_{k\in k} \ln(1+\Gamma_k) \tag{7}$$

The main objective is to enhance the RISs reflection-beamforming Φ, as well as AP-transmission beamforming V to maximize channel throughput while adhering to the total power constraint. The transmission/reflection beamforming design problem can be stated,

$$\mathcal{P}_0: \max_{\boldsymbol{\Phi},\mathbf{V}} \sum_{k\in|K|} \ln(1+\Gamma_k) \tag{8}$$

$$\text{s.t: } \boldsymbol{\Phi}_{r,n} \in \left\{0, \frac{\pi}{2^{b-1}}, \dots, \frac{(2^b-1)\pi}{2^{b-1}}\right\}, \ \forall r \in R, \forall n \in N \tag{8a}$$

$$\operatorname{tr}\left(\mathbf{V}_k \mathbf{V}_k^H\right) \leq P_{max} \tag{8b}$$

where P_{max} denotes the AP maximum allowed transmitting power. The reflecting element phase shift limitation is specified in the constraint of (8a). Owing to the restrictions in (8a) and (8b), the optimization issue presented in (8) is a significant complicated problem challenge; therefore, in the proposed scheme, and for the sake of simplification, we consider the maximum-ratio transmission for the actively transmit beamforming [27], [28].

$$\mathbf{V}^T = \frac{(\mathbf{G\Phi H} + \mathbf{F})^H}{\|\mathbf{G\Phi H} + \mathbf{F}\|} \tag{9}$$

Up to this end, $\mathcal{P}_0$ can be modified to the following problem,

$$\mathcal{P}1: \max_{\boldsymbol{\Phi}} \|\mathbf{G\Phi H} + \mathbf{F}\|^2 \tag{10}$$

$$\text{s.t: } \boldsymbol{\Phi}_{r,n} \in \left\{0, \frac{\pi}{2^{b-1}}, \dots, \frac{(2^b-1)\pi}{2^{b-1}}\right\}, \ \forall \mathrm{r} \in \mathrm{R}, \forall \mathrm{n} \in \mathrm{N} \tag{10a}$$

$$\operatorname{tr}\left(\mathbf{V}_k \mathbf{V}_k^H\right) \leq P_{max} \tag{10b}$$

3. DEEP NEURAL NETWORK STRUCTURE

The beamforming neural network (BF-Net) is trained to solve the transmitting beamforming problem directly (no iteration) to enhance the system's throughput. The training data sets are compiled via an exhaustive search (offline phase) of each channel realization to select a RIS beamforming vector that maximizes the entire system's throughput. After training, the scheme will be ready to guess the passive beamforming vector for any given input channel gains. The suggested structure for this beamforming neural network (abbreviated BF-Net for convenience of notation) consists of multiple layers, as illustrated in Figure 2.

The structure has 10 layers and preserves data at the dim, $\mathrm{NM} \times K \times 3$ input layer while recurring a dim, 1×K vector at the output. Each neural network input utilizes the real/imaginary portions of the wireless channel. Convolutional layers (layers 2 and 5) are being used to extract the characteristics hidden in the network input data, including 16 filters totaling 3×3 pixels in size. The bias and weights are propagated through the layer to extract features. Following these layers (i.e., convolutional layers), we already have normalization and activation layers, which provide a faster learning rate through normalization and optimal converging. On the other hand, the normalization layers, similar to dropout-layers, can moderate the over-fitting opportunity by offering some noise to the convolution layer. Next, the flattened layer will flatten the output of the convolutional layers to harvest a single feature vector of dim |K|. A rectified-linear unit activation function (ReLU) can be employed for the intermediate layers. In contrast, the last layer prefers the soft-max function to certify a good classification prediction.

$$ReLU(z) = Max\{0, z\} \tag{11}$$

$$Softmax(z) = \frac{e^{z_i}}{\sum_{j=1}^{K} e^{z_j}} \tag{12}$$

Where z is the layer input vector, this neural network is trained using stochastic-gradient descent (SG) for the optimized solution algorithms. For the output layer, as a regression loss (unsupervised method), the negative of the primary function in *P1* (objective), which samples (S) of training, can be defined,

$$loss = -\frac{1}{S}\sum_{s\in|S|} \|\mathbf{G}^s\,\mathbf{\Phi}^s\,\mathbf{H}^s + \mathbf{F}^s\|^2 \tag{13}$$

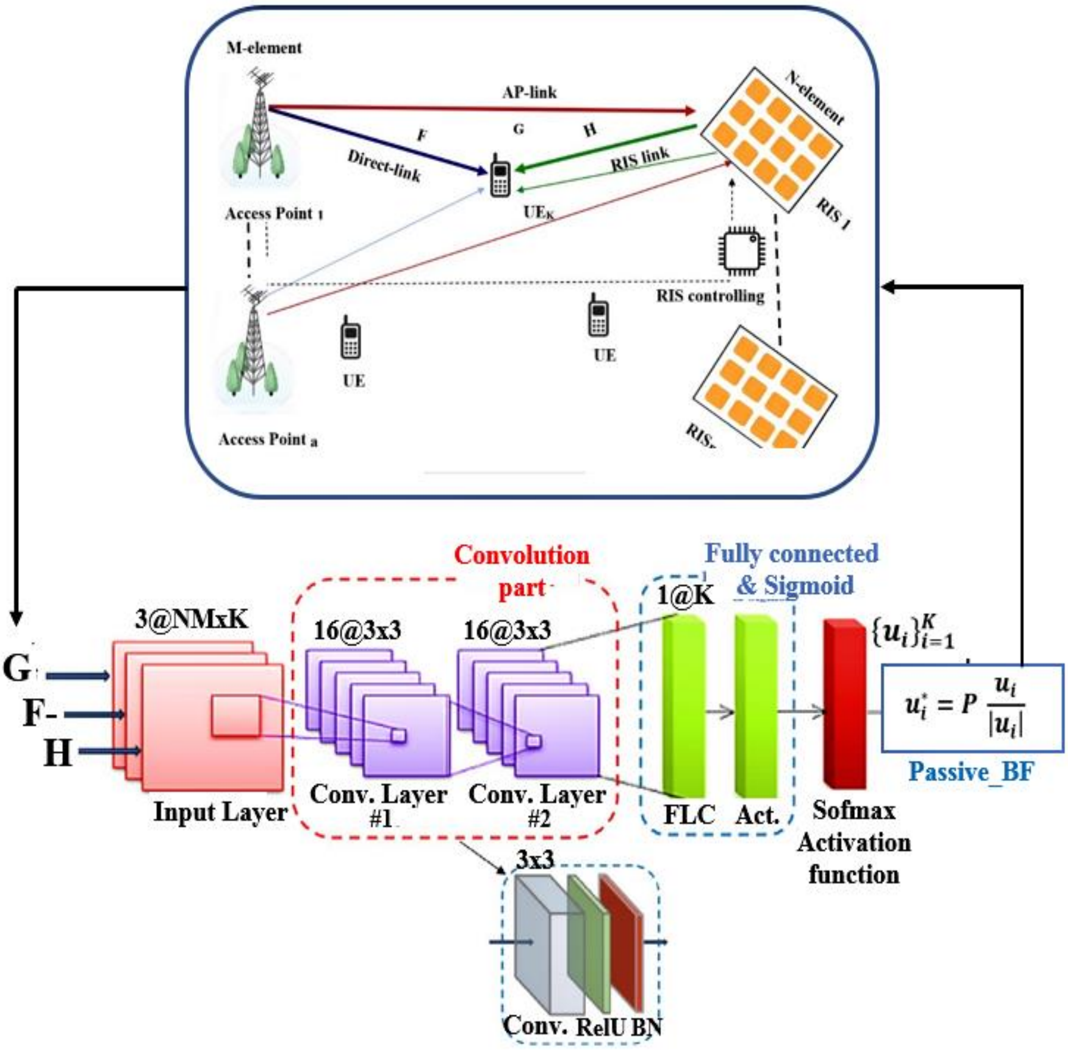

Figure 2. Structure of the proposed beamforming neural network

4. NUMERICAL RESULTS

Next, we will verify the proposed network's performance through numerical simulation. All parameters of the network and the baseline near-optimal algorithm for the sake of results comparison are indicated in Table 1 (otherwise are specified within the figures caption). First, we examine the effect of the RIS's element count on the per-user performance. As shown in Figure 3, both techniques' performance is close to each other and increases with the deployment of RIS elements. This plot shows that increasing the number of elements by 10 (from 20 up to 30) can improve the user throughput in the context by 18%. The proposed method achieves more than 95% of the optimal throughput value for the number of antennas of 4 and 30 RIS's elements at a low implementation cost compared to the optimal scheme.

Table 1. System parameters values are applied in the simulation

Parameter	Setting
Access point antenna number	$M_t = \{2, 4, 6, 10\}$
RIS elements number	N=8X8
Number of available users	$\|K\| = 4$
The budget of the transmit power	$P_{max} =$ 10 dB
AWGN noise power spectral density	$\sigma_n^2 =$ -174 dBm/Hz
Pathloss model	Pl(dB)=-126.1+36.5 log10 (distance)
Small-scale fading channels	Independent and identically distributed (i.i.d) Rayleigh
Train model of the neural network	0.001 learn rate Adam model
Epochs number	1,000
The benchmark scheme	An iterative semi-definite [27].

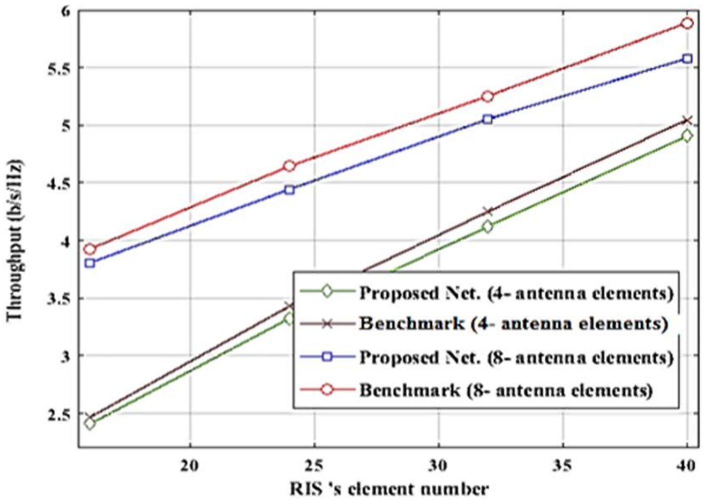

Figure 3. The effect of the RIS's element count on user throughput

Next, Figure 4 demonstrates the effect of the AP's antenna count on per-user throughput. The throughput of both methods rises with the amount of AP antenna and the development of RIS elements. Also, Figure 5 put together the effect of the number of AP antennas and the RIS's elements number on the user throughput. As expected, the proposed system beamforming gets better with the deployment of more elements of antennas and RIS reflectors. Also, it outperforms the benchmark performance overall in the range of the x and y-axis. Lastly, Figure 6 introduces a compression between the proposed and the benchmark schemes in terms of time-performance, i.e., the average time-complexity when there are 10 antenna elements at the AP. It is worth mentioning that the training stage of the proposed deep NN is carried out offline. Hence, we emphasize the time-complexity results of the online prediction stage. In this regard, the big-O symbol, i.e., "order of," can be used to introduce the time-complexity of a specific procedure. Both input and flatten layers have a simple complexity that can ignore the time cost. For filters of the dimension $n_j \times n_j$ in the j-*th* convolution layer with convolution output size of $x_j \times y_j$, there are the same number of addition and multiplication where in this case the multiplication complexity is of the order,

$$O\left(\sum_{j=1}^{L} n_j\, y_j \,.\, n_j\, x_j \,.\, f_j\, f_{j-1}\right) \tag{14}$$

where $f_j\, f_{j-1}$ denote the number of the convolution filters in the j-*th* and *(j-1)*-*th* layers, respectively. In addition, the complexity of additions is insignificant if compared to that associated with the multiplications. Also, since the rectified linear activation function (ReLU) defines the input sample's sign only, the complexity can be neglected.

Yet, for the BN-layer and the total activation layers, the order is $O(\sum_{j=1}^{L} y_j\ x_j\ f_j)$. Assuming that FLC-layer has z-neurons, then the order will be as follows, $O(\sum_{j=1}^{L} z\,.\,y_{FLC}\ x_{FLC}\ f_{FLC})$. We employ zero-padding of size one for our proposed NN, and we have 16 convolution filters of dimension 3×3; then the convolution output is of size $2 \times KNM$, and the total complexity will be approximate, of the order, $O(KNM)$. It is clear from Figure 6 the superior of the proposed scheme in compression to the great complexity of the iterative sub-optimal precoding method, e.g., for 25 RIS's elements, the average consumed time is about 0.851×10^{-3} sec, while for the baseline algorithm, the average required time is about 4.862×10^{-3} sec.

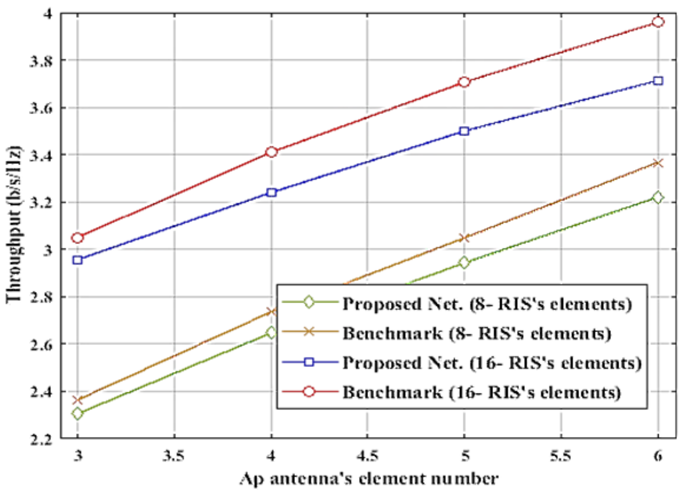

Figure 4. The effect of the number of AP antennas on user throughput

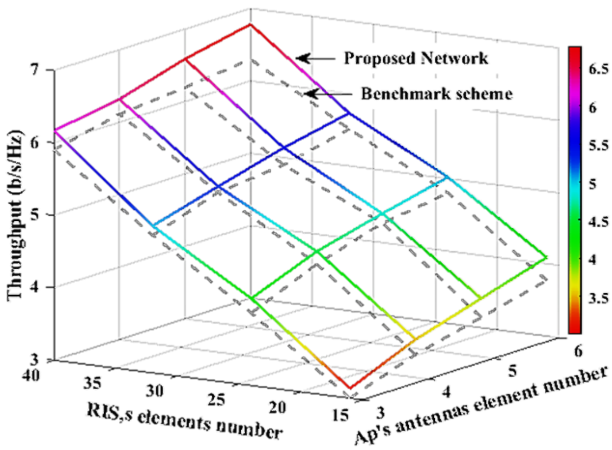

Figure 5. The effect of both AP antennas number/RIS's elements number on the user throughput

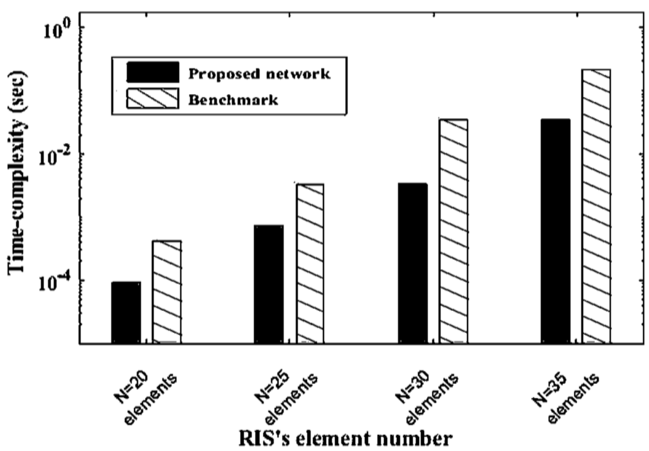

Figure 6. The average time required by the algorithms concerning the number of RIS items

5. CONCLUSION

We consider optimizing RIS beamforming to increase the users' throughput in this study. We offer unsupervised/deep neural network (U/DNN) based on convolutional neural networks (CNNs) to reduce the training weights and number to deal with the non-convexity issue. By engaging with the wireless communication environment and obtaining real-time data, the RIS controller developed a policy for optimizing the RIS's phase shift. The simulation results show that both techniques' performance is close to each other while increasing with the deployment of RIS passive elements and AP antenna numbers. The average consumed time when the AP has 10 antenna elements, it is evident that the technique is better in compression with the iterative sub-optimal precoding strategy's excessive complexity.

REFERENCES

[1] A. Taha, M. Alrabeiah, and A. Alkhateeb, "Enabling large intelligent surfaces with compressive sensing and deep learning," *IEEE Access*, vol. 9, pp. 44304–44321, 2021, doi: 10.1109/ACCESS.2021.3064073.

[2] M. Di Renzo *et al.*, "Smart radio environments empowered by reconfigurable AI meta-surfaces: an idea whose time has come," *EURASIP Journal on Wireless Communications and Networking*, no. 1, Dec. 2019, doi: 10.1186/s13638-019-1438-9.

[3] F. Keti, S. M. Atroshey, and J. A. Hamadamin, "Spectral and energy efficiencies maximization in downlink NOMA systems," *Bulletin of Electrical Engineering and Informatics*, vol. 11, no. 3, pp. 1449–1459, Jun. 2022, doi: 10.11591/eei.v11i3.3654.

[4] D. P. Mishra, K. K. Rout, and S. R. Salkuti, "Compact MIMO antenna using dual-band for fifth-generation mobile communication system," *Indonesian Journal of Electrical Engineering and Computer Science (IJEECS)*, vol. 24, no. 2, pp. 921–929, Nov. 2021, doi: 10.11591/ijeecs.v24.i2.pp921-929.

[5] H. F. Rashag and M. H. Ali, "Optimization of transmission signal by artificial intelligent," *International Journal of Advances in Applied Sciences*, vol. 8, no. 4, pp. 290–292, Dec. 2019, doi: 10.11591/ijaas.v8.i4.pp290-292.

[6] A. M. Elbir, A. Papazafeiropoulos, P. Kourtessis, and S. Chatzinotas, "Deep channel learning for large intelligent surfaces aided mm-wave massive MIMO systems," *IEEE Wireless Communications Letters*, vol. 9, no. 9, pp. 1447–1451, Sep. 2020, doi: 10.1109/LWC.2020.2993699.

[7] C. Huang *et al.*, "Holographic MIMO surfaces for 6G wireless networks: opportunities, challenges, and trends," *IEEE Wireless Communications*, vol. 27, no. 5, pp. 118–125, Oct. 2020, doi: 10.1109/MWC.001.1900534.

[8] D. Dardari, "Communicating with large intelligent surfaces: fundamental limits and models," *IEEE Journal on Selected Areas in Communications*, vol. 38, no. 11, pp. 2526–2537, Nov. 2020, doi: 10.1109/JSAC.2020.3007036.

[9] C. Huang, A. Zappone, G. C. Alexandropoulos, M. Debbah, and C. Yuen, "Reconfigurable intelligent surfaces for energy efficiency in wireless communication," *IEEE Transactions on Wireless Communications*, vol. 18, no. 8, pp. 4157–4170, Aug. 2019, doi: 10.1109/TWC.2019.2922609.

[10] M. A. ElMossallamy, H. Zhang, L. Song, K. G. Seddik, Z. Han, and G. Y. Li, "Reconfigurable intelligent surfaces for wireless communications: principles, challenges, and opportunities," *IEEE Transactions on Cognitive Communications and Networking*, vol. 6, no. 3, pp. 990–1002, Sep. 2020, doi: 10.1109/TCCN.2020.2992604.

[11] A. Kansal and P. Singh, "Performance improvement of MU-MIMO system by optimizing the K-Factor for the K-Mean user grouping algorithm," *International Journal of Informatics and Communication Technology (IJ-ICT)*, vol. 5, no. 3, pp. 89–93, Dec. 2016, doi: 10.11591/ijict.v5i3.pp89-93.

[12] H. Huang, W. Xia, J. Xiong, J. Yang, G. Zheng, and X. Zhu, "Unsupervised learning-based fast beamforming design for downlink MIMO," *IEEE Access*, vol. 7, pp. 7599–7605, 2019, doi: 10.1109/ACCESS.2018.2887308.

[13] X. Li and A. Alkhateeb, "Deep learning for direct hybrid precoding in millimeter wave massive MIMO systems," in *2019 53rd Asilomar Conference on Signals, Systems, and Computers*, Nov. 2019, pp. 800–805, doi: 10.1109/IEEECONF44664.2019.9048966.

[14] Z. Qin, H. Ye, G. Y. Li, and B.-H. F. Juang, "Deep learning in physical layer communications," *IEEE Wireless Communications*, vol. 26, no. 2, pp. 93–99, Apr. 2019, doi: 10.1109/MWC.2019.1800601.

[15] J. Gao, M. R. A. Khandaker, F. Tariq, K.-K. Wong, and R. T. Khan, "Deep neural network based resource allocation for V2X communications," in *2019 IEEE 90th Vehicular Technology Conference (VTC2019-Fall)*, Sep. 2019, pp. 1–5, doi: 10.1109/VTCFall.2019.8891446.

[16] M. Cui, G. Zhang, and R. Zhang, "Secure wireless communication via intelligent reflecting surface," *IEEE Wireless Communications Letters*, vol. 8, no. 5, pp. 1410–1414, Oct. 2019, doi: 10.1109/LWC.2019.2919685.

[17] H. Shen, W. Xu, S. Gong, Z. He, and C. Zhao, "Secrecy rate maximization for intelligent reflecting surface assisted multi-antenna communications," *IEEE Communications Letters*, vol. 23, no. 9, pp. 1488–1492, Sep. 2019, doi: 10.1109/LCOMM.2019.2924214.

[18] H. Sun, X. Chen, Q. Shi, M. Hong, X. Fu, and N. D. Sidiropoulos, "Learning to optimize: training deep neural networks for interference management," *IEEE Transactions on Signal Processing*, vol. 66, no. 20, pp. 5438–5453, Oct. 2018, doi: 10.1109/TSP.2018.2866382.

[19] C. Huang, G. C. Alexandropoulos, C. Yuen, and M. Debbah, "Indoor signal focusing with deep learning designed reconfigurable intelligent surfaces," in *2019 IEEE 20th International Workshop on Signal Processing Advances in Wireless Communications (SPAWC)*, Jul. 2019, pp. 1–5, doi: 10.1109/SPAWC.2019.8815412.

[20] J. Gao, C. Zhong, X. Chen, H. Lin, and Z. Zhang, "Unsupervised learning for passive beamforming," *IEEE Communications Letters*, vol. 24, no. 5, pp. 1052–1056, May 2020, doi: 10.1109/LCOMM.2020.2965532.

[21] H. Song, M. Zhang, J. Gao, and C. Zhong, "Unsupervised learning-based joint active and passive beamforming design for reconfigurable intelligent surfaces aided wireless networks," *IEEE Communications Letters*, vol. 25, no. 3, pp. 892–896, Mar. 2021, doi: 10.1109/LCOMM.2020.3041510.

[22] W. Lee, M. Kim, and D.-H. Cho, "Transmit power control using deep neural network for underlay device-to-device communication," *IEEE Wireless Communications Letters*, vol. 8, no. 1, pp. 141–144, Feb. 2019, doi: 10.1109/LWC.2018.2864099.

[23] T. Lin and Y. Zhu, "Beamforming design for large-scale antenna arrays using deep learning," *IEEE Wireless Communications Letters*, vol. 9, no. 1, pp. 103–107, Jan. 2020, doi: 10.1109/LWC.2019.2943466.

[24] I. Al-Shaeli and I. Hburi, "An efficient beamforming design for reflective intelligent surface-aided communications system," in

2022 International Conference on Computer Science and Software Engineering (CSASE)*, Mar. 2022, pp. 151–156, doi: 10.1109/CSASE51777.2022.9759797.

[25] Q. Wu and R. Zhang, "Towards smart and reconfigurable environment: intelligent reflecting surface aided wireless network," *IEEE Communications Magazine*, vol. 58, no. 1, pp. 106–112, Jan. 2020, doi: 10.1109/MCOM.001.1900107.

[26] I. Hburi, H. F. Khazaal, R. Fahdel, and H. Raadi, "Sub-array hybrid beamforming for sustainable largescale mmWave-MIMO communications," in *2021 International Conference on Advanced Computer Applications (ACA)*, Jul. 2021, pp. 101–106, doi: 10.1109/ACA52198.2021.9626806.

[27] I. S. Baqer, "A practical weighted sum rate maximisation for multi-stream cellular MIMO systems," in *2018 International Conference on Engineering Technology and their Applications (IICETA)*, May 2018, pp. 48–53, doi: 10.1109/IICETA.2018.8458083.

[28] D. Tse and P. Viswanath, *Fundamentals of wireless communication*. Cambridge University Press, 2005.

BIOGRAPHIES OF AUTHORS

Intisar AL-Shaeli received the B.Eng. degree in control and system engineering from University of Technology, Iraq, in 2002. Currently, she is an MSc student at the Department of Electrical Engineering, Wasit University. She is employee in the Ministry of Communication in Iraq, Informatics and Telecommunications Public Company as chief engineering officer. Here research interests in the field of wireless communication and telecommunication in addition to computer control. She can be contacted at email: intisark302@uowasit.edu.iq.

Ismail Sharhan Hburi received the B.Eng. and M.Sc. degrees from the University of Technology, Baghdad, Iraq, in 1991 and 2007, respectively, the Ph.D. degree in wireless communication from Brunel University London, U.K., in 2017. His current research area is wireless communication, massive MIMO cellular networks, IoT, wireless sensor networks. He can be contacted at email: isharhan@uowasit.edu.iq.

Ammar A. Majeed received the B.eng. degree in electrical engineering from university of Wasit in 2016. Now, he is M.S student in the same university. He is a technical engineer in Middle Technical University, Kut Technical Institute. His research field is wireless communication systems, massive MIMO cellular systems. He can be connected at email: ammara302@uowasit.edu.iq.